Chemistry & Biology, Vol. 9, 619–628, May, 2002, ©2002 Elsevier Science Ltd. All rights reserved. PII S1074-5521(02)00141-2

A Selected Ribozyme Catalyzing Diverse Dipeptide Synthesis

Lele Sun,[1] Zhiyong Cui,[1] Robert L. Gottlieb,[2] and Biliang Zhang[1,3]
[1]Program in Molecular Medicine
University of Massachusetts Medical School
Worcester, Massachusetts 01605
[2]Department of Chemistry and Biochemistry
University of Colorado at Boulder
Boulder, Colorado 80309

Summary

The sequence of events by which protein, RNA, and DNA emerged during early biological evolution is one of the most profound questions regarding the origin of life. The contemporary role of aminoacyl-adenylates as intermediates in both ribosomal and nonribosomal peptide synthesis suggests that they may have served as substrates for uncoded peptide synthesis during early evolution. We report a highly active peptidyl transferase ribozyme family, isolated by in vitro selection, that efficiently catalyzes dipeptide synthesis by using an aminoacyl-adenylate substrate. It was characterized by sequence and structural analysis and kinetic studies. Remarkably, the ribozyme catalyzed the formation of 30 different dipeptides, the majority of rates being within 5-fold that of the Met-Phe dipeptide required by the selection. The isolation of this synthetic ribozyme fosters speculation that ribozyme-mediated uncoded peptide synthesis may have preceded coded peptide synthesis.

Introduction

The "RNA world" hypothesis proposes that RNA carried out both genomic and catalytic functions during an early stage in the evolution of life [1–5]. If an "RNA world" was a precursor to extant life, RNA must have been able both to catalyze RNA replication and to direct peptide synthesis, then and now [6–8]. A recent report described a ribozyme that catalyzes RNA polymerization by the successive addition of up to 14 nucleotides and can use any sequence of RNA for its template [9]. This provides further evidence for the plausibility of RNA-catalyzed RNA replication. The evolution of RNA-catalyzed coded protein synthesis would have been a critical step in the transition from the RNA world to modern biological systems [10, 11].

The aminoacyl-adenylate is a universal intermediate for both ribosomal and nonribosomal processes of peptide biosynthesis in modern biological systems [12–14]. In coded peptide synthesis, the specific amino acid is activated as its aminoacyl-5′-adenylate en route to the formation of the appropriate 3′(2′)-aminoacyl-tRNA. The tRNA provides the amino acid with a nucleic acid "tag," although such a tag would not be required by uncoded peptide synthesis machines. Nonribosomal polypeptide biosynthesis requires a minimum of three successive steps: (1) amino acid adenylation (aa-AMP), (2) aminoacylation of holo-PCP (Peptide Carrier Protein) by the formation of a thioester, and (3) peptide bond formation. Thus, the aminoacyl-adenylate is the key activated intermediate for both types of polypepetide biosynthesis.

Before the emergence of coded peptide synthesis, how were peptides made? What biological molecule was the first catalyst for peptide synthesis? From the demonstration that RNA can form an aminoacyl-5′-guanylate-RNA [15], we can make the feasible extrapolation that the biologically relevant aminoacyl-5′-adenylates could have been present in a hypothesized primordial RNA world in which ribozymes were a major catalytic force. Using the aminoacyl-adenylate as substrate, researchers have isolated self-aminoacylating ribozymes from combinatorial RNA libraries [16–18]. Furthermore, RNAs capable of catalyzing amide bond formation have been isolated with biotinyl-5′-AMP phosphoanhydride [19] or a nucleotide-aminoacyl ester as a substrate [20].

We previously isolated ribozymes that catalyze peptide bond formation by employing a substrate of predominantly *N*-blocked methionyl-3′(2′)-AMP esters [21] (the numbering convention in this manuscript denotes the site of chemical ligation between adenosine-5′-monophosphate and the indicated acyl side chain; thus acyl-3′(2′)-AMP refers to esters of adenosine-5′-monophosphate, whereas acyl-5′-AMP refers to the mixed phosphoanhydride). The 5′-monophosphoryl-adenosine-3′(2′)-*O*-(*N*-biotinylamidocaproyl-methionyl ester (the bitonylamidocaproyl group is abbreviated to biotin or Bio in this manuscript; Bio-Met-3′(2′)-AMP) was prepared by Gottikh's method [22], with carbonyl diimidazole (CDI) serving to activate the amino acid by forming an aminoacyl-imidazolide intermediate. Lacey et al. [23] have made extensive use of this reaction for the preparation and study of aminoacyl nucleotide esters. The major product of *N*-acetyl aminoacyl imidazolides reacted with AMP is the 3′(2′)-aminoacyl-AMP monoester, but AMP-2′,3′-aminoacyldiester and aminoacyl-5′-AMP anhydride are also formed [24]. We will report elsewhere (R.L.G., Z.C., L.S., B.Z., and T. Cech, unpublished data; Z.C., L.S., and B.Z., unpublished data) that the previously characterized clone 25 ribozyme is in fact active with the *N*-Bio-aminoacyl-5′-adenylate, but does not appear to be active with the Bio-Met-3′(2′)-AMP substrate as had been reported previously [21]. In the present study, we took a pool from the previous selection and applied additional selection pressure with pure *N*-Bio-aminoacyl-5′-adenylate as the substrate.

Here, we report the identification of peptide-synthesizing ribozymes that use *N*-Bio-aminoacyl-5′-adenylate as a substrate for selecting peptide-synthesizing ribozymes. We have identified one highly active ribozyme family that can catalyze dipeptide synthesis with six different aminoacyl-5′-adenylates and five different RNA-tethered amino acids; the amino acids used in the selection are replaced with other standard amino acids.

[3]Correspondence: biliang.zhang@umassmed.edu

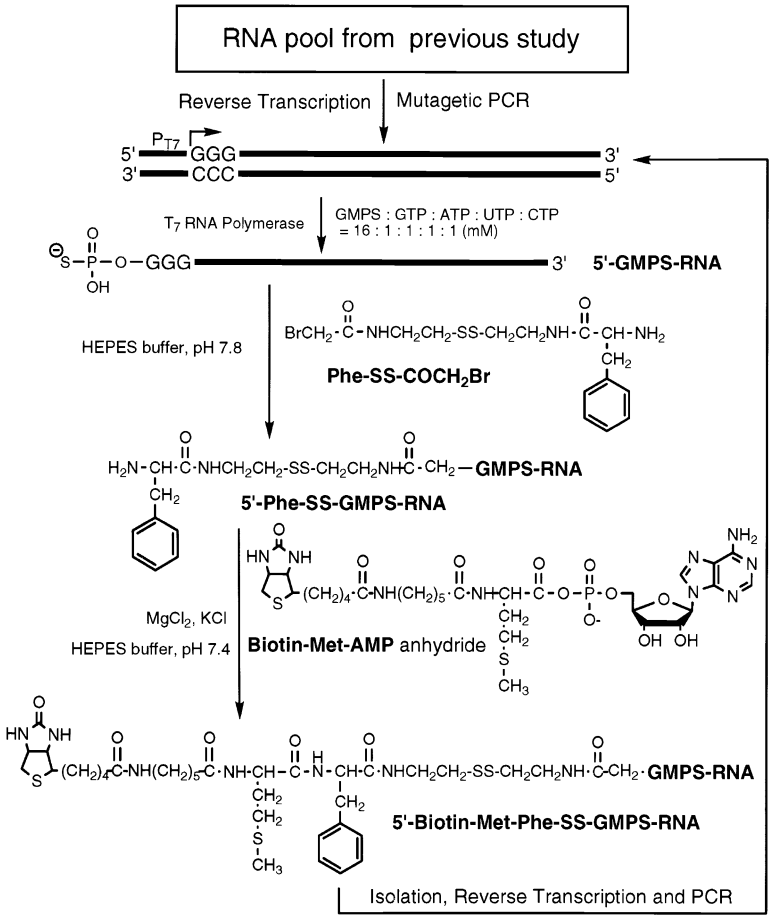

Figure 1. Initial RNA Pool Construction and In Vitro Selection

The starting RNA pool was from the tenth generation of the previous work [21]. The DNA was prepared by RT-PCR with the following primers. The 5′-primer was 5′-AGCGAATTC TAATACGACTCACTATAGGGAGAGACCTG CCATTCAC-3′; the 3′-primer was 5′-CACGG ATCCTGACGCTGCTT-3′. The RNA pool was prepared from PCR-amplified DNA by in vitro transcription in the presence of GMPS:GTP = 8:1. The 5′-GMPS-RNA was purified by PAGE and then reacted with *N*-bromoacetyl-*N*′-phenylalanyl-cystamine. The 5′-Phe-SS-RNA was incubated with Biotin-Met-AMP in the presence of $MgCl_2$, KCl, and HEPES buffer, and the reacted 5′-Biotin-Met-Phe-SS-RNA molecules were isolated by collection on streptavidin-agarose, washed in the presence of urea, and resolubilized by the addition of DTT. The collected RNA was used as RT-PCR templates for input into the next cycle of selection.

This new system bolsters the case that RNAs of antiquity could have catalyzed uncoded protein synthesis with aminoacyl-5′-adenylates, compounds that persist as intermediates for both uncoded and coded peptide synthesis in biology today.

Results and Discussion

In Vitro Selection

Additional rounds of in vitro selection beginning with the 10th-generation RNA pool described previously [21] were performed. The initial selection pressure had been applied with a substrate consisting of predominantly biotinoyl-amidocaproyl-methionyl-3′(2′)-AMP esters (Bio-Met-3′(2′)-AMP) [21]. Six additional rounds of selection were now carried out, with a switch to the *N*-biotinyl-amidocaproyl-methionyl-5′-adenylate (Bio-Met-5′-AMP, synthesized as described for its congeners in reference [25] with modification) as the selection substrate.

The selection reaction of 5′-Phe-SS-GMPS-RNA with Bio-Met-5′-adenylate is outlined in Figure 1. The in vitro-transcribed 5′-GMPS-RNA pool transcribed from the 10th-generation DNA templates was reacted with *N*-bromoacetyl-*N*′-phenylalanyl-cystamine to produce 5′ phenylalanyl-cystaminyl-acetamidyl-GMPS-RNA (5′-Phe-SS-GMPS-RNA) and incubated with biotin-Met-5′-AMP phosphoanhydride in 100 mM $MgCl_2$, 300 mM KCl, and 50 mM HEPES buffer (pH 7.4) at 25°C. The active RNA molecules were isolated by streptavidin-agarose, washed extensively in the presence of urea, and subsequently resolubilized as described [21]. Reverse transcription and amplification by mutagenic PCR were performed for the first three cycles of the selection that used biotin-Met-5′-AMP. After six cycles of selection with biotin-Met-5′-AMP (sixteen total cycles of selection), the final pool was cloned and sequenced.

A highly active ribozyme family was identified by assaying individual clones coupled with sequence alignment analysis. This family comprised six RNAs: R180, R182, R185, R186, R193, and R202. We re-isolated two clones, R185 and R193, that were identical to clones 71 and 27, respectively [21]. Fortuitously, we also found eight more family members that emerged from the background of a separate selection that was intended to isolate variants of the distinct clone 16 and 25 ribozyme families [21]. These fourteen ribozyme sequences are shown in Figure 2A. The sequence between G25 and G127 was a highly conserved region. The region after U128 of the family has a significantly divergent sequence (pink box, Figure 2A). These data suggest that within the internal sequence of the ribozyme, the 5′-proximal portion is more critical for activity than its more distal sequence; unfortunately, the relative importance of the 5′ and 3′ termini could not be assessed by comparative sequence analysis because they were constrained to form primer binding sites.

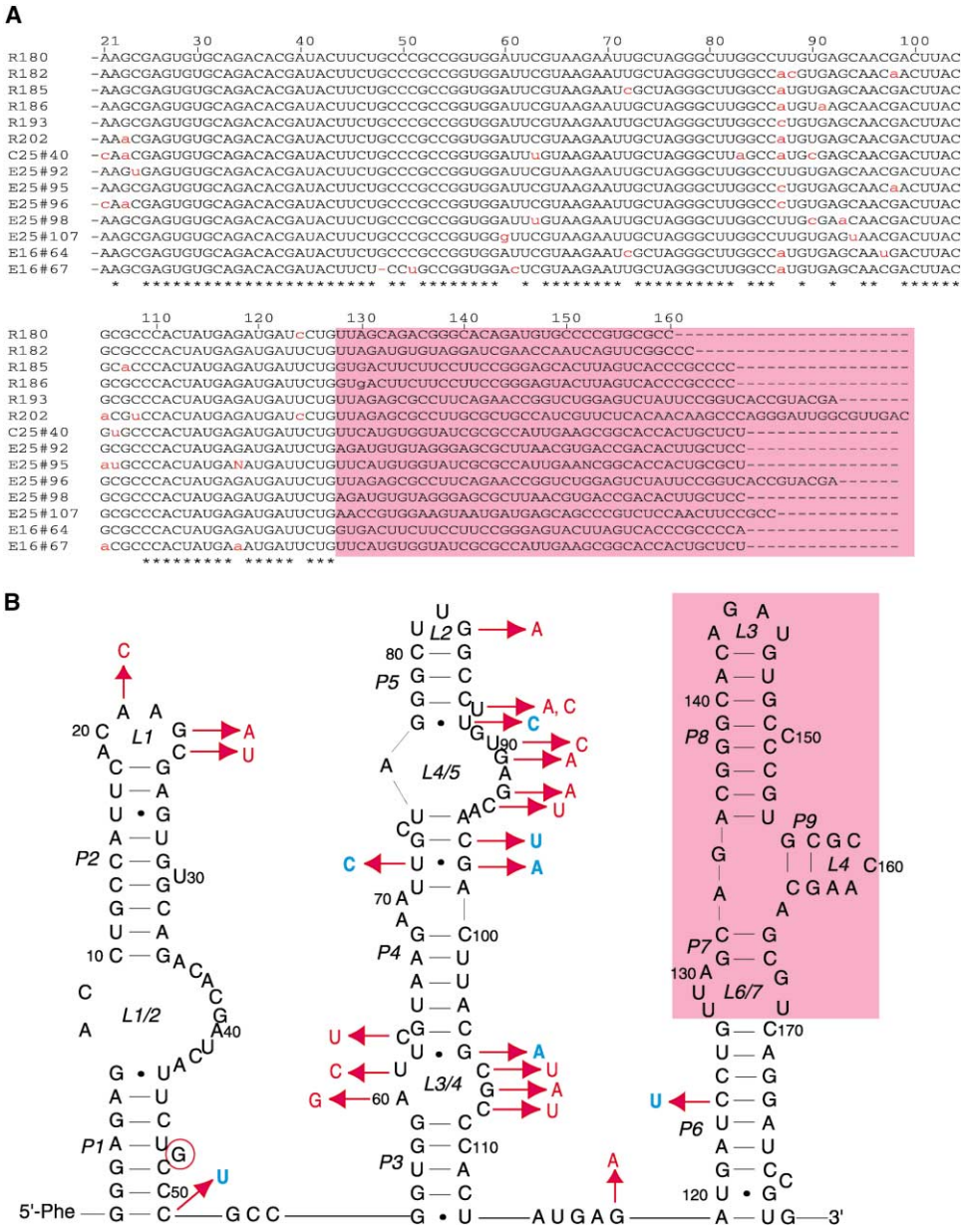

Figure 2. The Sequences and Secondary Structural Model of the R180 Ribozyme Family

The red box indicates the region of significant divergence within the family.

(A) Sequence alignment of the R180 ribozyme family. The flanking fixed primer sequences are not shown. Differences in individual clones from the consensus sequence (top sequence) are in lowercase and red-colored letters.

(B) Secondary structural model of the R180 ribozyme and its phylogenetic family. A deleted nucleotide is encircled. The single-nucleotide variations that fall within predicted loops (red) and base-paired regions (blue) in the phylogenetically conserved regions are highlighted. The pink box indicates the region of structural divergence within the family.

Secondary Structure of the R180 Ribozyme

The sequences of six RNAs were analyzed by the RNA Mfold program [26] to predict their secondary structures. The best secondary-structural model of the R180 ribozyme, illustrated in Figure 2B, was obtained by comparison with all secondary-structural models of these fourteen ribozymes. The other thirteen ribozymes fit this secondary-structural model as well. Twenty-three nucleotide positions within the highly conserved regions of the R180 ribozyme were variable in other members of the family. Sixteen phylogenetic variations were located within predicted loop regions. Those seven variant positions that fall within predicted base pairs all preserve Watson-Crick or G•U wobble-matched base pairs. For example, the G1:C50 Watson-Crick base pair that closes P1 in the R180 ribozyme was a G1•U51 wobble base pair in the E16#67 ribozyme. Similarly, the U62•G105 wobble base pair within P4 in the R180 ribozyme was a U62:A105 Watson-Crick base pair in R202, E16#67, and E25#95 ribozymes. The fourteen ribozymes fit this

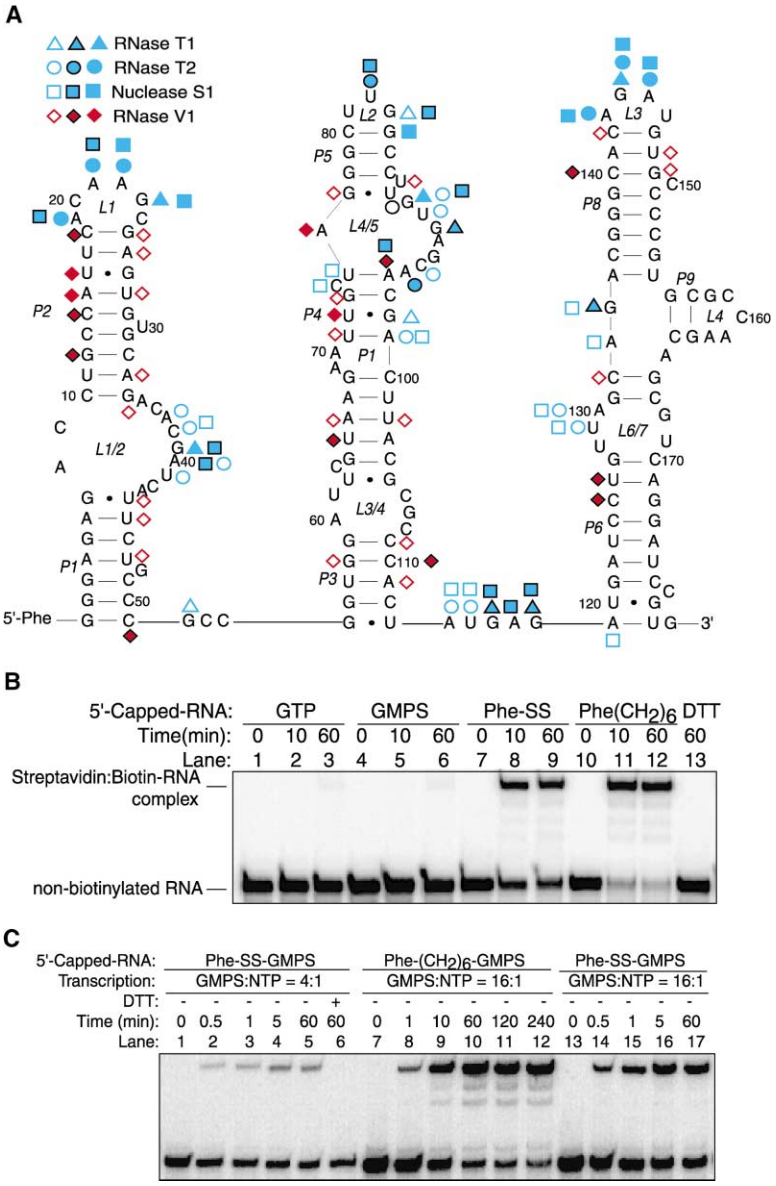

Figure 3. Secondary-Structural Analysis and Peptidyl Transferase Reactions of the R180 Ribozyme

(A) Enzymatic probing of the secondary structure of the R180 ribozyme. The shaped symbols superimposed on the structure show positions cleaved by specific nucleases: RNase T1 (triangle), RNase T2 (circle), nuclease S1 (square), and RNase V1 (diamond); solid color, filled color, and open symbols represent strong, medium, and weak enzymatic cleavage, respectively.

(B) Autoradiogram of the products of the peptide bond-forming reaction between 5′-capped RNAs and biotin-Met-5′-AMP anhydride as detected by a streptavidin band-shift assay. RNA was prepared by in vitro transcription either with GTP alone (GTP lanes) or with a ratio of GMPS:GTP = 16:1. The GMPS-containing RNAs were used either without further reaction (GMPS lanes) or after the installation of a phenylalanyl residue on a linker containing an internal disulfide bond (Phe-SS lanes) or lacking a disulfide bond [Phe(CH_2)$_6$ lanes]. The reactions were performed with 2 μM 5′-capped RNA (R180) and 50 μM biotin-Met-AMP in 300 mM KCl, 100 mM $MgCl_2$, and 50 mM HEPES buffer (pH 7.4) at 25°C. Lane 13 is the same as lane 9 but was treated with DTT. The bottom bands are the unreacted RNA, and the top bands are the streptavidin:biotinyl-RNA complex.

(C) Autoradiogram of the peptide bond-forming reaction of 5′-Phe-SS-GMPS-RNA with biotin-Met-AMP anhydride. RNA was prepared with the indicated ratios of GMPS to GTP.

secondary-structural model very well until they diverge drastically (pink box, Figure 2B) prior to reconverging for the final 20 nucleotide fixed primer binding site. This area of primary sequence diversion generated inconsistent secondary structures in different members of the family, suggesting that this variable region may not be structurally or functionally important.

The structural model predicts nine stem helices (P1–P9), four internal loops (L1/2, L3/4, L4/5, and L6/7), four hairpin loops (L1–L4), and one three-way junction (J7/8/9). The secondary structure of the R180 ribozyme was probed by nuclease digestion experiments with single strand-specific nuclease S1, RNase T1, RNase T2, and double strand-specific RNase V1 (Figure 3A). The nuclease digestion products were resolved by subjecting them to 20% polyacrylamide gel electrophoresis (PAGE). The enzymatic probing results are summarized in Figure 3A. The guanine nucleotides in the hypothesized internal loops and single-stranded regions (G39, G52, G89, G91, G116, G118, and G134) as well as in the hairpin loops (G23, G83, and G144) were cleaved by single strand-specific RNase T1. The strong cutting patterns generated by single strand-specific RNase T2 (A19, A21, A22, A37, C38, A40, U41, U82, G89, U90, C94, A95, A114, U115, U129, A130, A143, G144, and A145) correlated well with the predicted internal loops, hairpin regions, and bulge regions. The predicted single-stranded positions at A19, A21, A22, G23, C38, G39, A40, U82, G83, G89, G116, G118, A143, G144, and A145 were strongly cleaved by nuclease S1. The cleavage sites of double strand-specific RNase V1 correlated with the helical P1, P2, P3, P4, P5, P6, and P8 regions of the secondary-structural model. The RNase V1 cleavage positions located on both sides of the P2, P3, P4, and P8 helices provided evidence that these regions are double stranded. With the exception of one putative double-stranded region of P4 that was also cleaved by single strand-specific nucleases, the nuclease digestion

results agree well with the secondary-structural model of the R180 ribozyme (Figure 3A).

Ribozyme-Mediated Reactions and Product Validation

Several control reactions were carried out to validate the ribozyme-mediated formation of a peptide bond. These reactions were monitored by streptavidin gel-shift electrophoresis (Figures 3B and 3C). The installation of the nucleophilic Phe residue onto the 5′-end of a 5′-GMPS-capped ribozyme is achieved by sulfur-selective attack on a bromoacetyl-activated Phe-containing linker. To verify that the peptidyl transferase reaction was dependent on the presence of the aminoacyl-containing linker, we transcribed a 5′-GTP-capped RNA from the R180 cDNA. Treatment of 5′-GMPS- and 5′-GTP-initiated R180 RNAs with the same Phe-containing linker reagent should yield the successfully modified 5′-Phe-SS-GMPS-RNA and unmodified 5′-GTP-RNA, respectively. When the linker-exposed 5′-GTP-RNA was incubated with biotin-Met-5′-AMP anhydride under the same reaction conditions as those of 5′-Phe-SS-GMPS-RNA, no new band was formed (lanes 1–3, Figure 3B). When 5′-GMPS-RNA (R180) without phenylalanine linked to its 5′ end was incubated with biotin-Met-AMP anhydride, again no product was observed (lanes 4–6, Figure 3B). Together, these two negative controls demonstrate that the ribozyme-catalyzed peptidyl transferase reaction requires a 5′-GMPS-capped RNA that has been matured by covalent modification with the Phe-containing linker.

When 5′-Phe-SS-GMPS-RNA (R180) was incubated with biotin-Met-AMP, a new band was formed at an approximate 50% yield at the reaction's final extent (lanes 7–9, Figure 3B; lanes 13–17, Figure 3C). A non-cleavable linker in which two sulfur atoms were replaced by two methylene groups was prepared [Phe-$NH(CH_2)_6NH$-$C(O)CH_2Br$]. Incubation of 5′-Phe-$NH(CH_2)_6NHC(O)CH_2$-GMPS-RNA (R180) with biotin-Met-5′-AMP anhydride resulted in formation of the product in about 80% yield at the reaction's final extent (lanes 10–12, Figure 3B; lanes 7–12, Figure 3C). This indicates that the majority of RNA molecules can be folded into a uniform active conformation. This result also suggests that the coupling efficiency of Phe-$NH(CH_2)_6NHC(O)CH_2Br$ with 5′-GMPS-RNA is greater than that of Phe-$NHCH_2CH_2SSCH_2CH_2NHC(O)CH_2Br$ because both were prepared from the same 5′-GMPS-RNA transcript. The transcription reaction conditions partially explain the observed incomplete reaction extent. The 5′-GMPS-RNA transcript was generated in the presence of both GMPS and GTP (molar ratio = 16:1), resulting in the occasional incorporation of GTP at the 5′ terminus rather than the desired GMPS as a stochastic event. Because the GTP-capped fraction of the predominantly GMPS-capped RNA cannot be conjugated to the Phe-linker, the anticipated 5′-heterogeneity of the "GMPS-RNA" is expected to prevent complete reaction. Consistent with this prediction, Figure 3C shows the time course of the peptide bond-forming reactions by three R180 ribozymes with different linkers and RNAs. The yield at the final reaction extent was only 25% for 5′-Phe-SS-GMPS-RNA that was made from a 5′-GMPS-RNA transcript with a GMPS:NTP ratio of 4:1 (lanes 1–6, Figure 3C) and 50% for a ratio of 16:1 (lanes 13–17, Figure 3C). The observed rate constant with 50 μM biotin-Met-AMP was 0.18 min^{-1} for 5′-Phe-$NH(CH_2)_6NHC(O)CH_2$-GMPS-RNA (lanes 7–12, Figure 3C) and 0.82 min^{-1} for 5′-Phe-SS-GMPS-RNA. The reaction rate of 5′-Phe-$NH(CH_2)_6NHC(O)CH_2$-GMPS-RNA is about 5-fold slower than that of 5′-Phe-SS-GMPS-RNA, although as noted earlier, a larger fraction of this RNA reacts. After treatment with dithiothreitol (DTT), the product band disappeared in the case of 5′-Phe-SS-GMPS-RNA (lane 13, Figure 3B; lane 6, Figure 3C) but not in the case of its 5′-Phe-$NH(CH_2)_6NHCOCH_2$-RNA congener in which the disulfide has been replaced with two methylene groups (data not shown), indicating that the coupled biotin was located at an RNA-distal position (i.e., on the phenylalanine side of the disulfide bond) of 5′-Phe-SS-GMPS-RNA.

In order to characterize further the ribozyme-catalyzed product, we isolated the product by reverse-phase high-performance liquid chromatography (RP-HPLC) and performed electrospray-ionization mass spectrometry (ESI-MS). We carried out a scaled-up reaction of 5′-Phe-SS-GMPS-RNA reacted with biotin-Met-5′-AMP anhydride to obtain enough material for LC-MS analysis. Treatment of the biotinylated RNA product with DTT released biotin-Met-Phe-cysteamine from the RNA, and the putative dipeptide was then subjected to LC-MS analysis. The biotin-Met-Phe-cysteamine had a retention time of 27.6 min by HPLC and two mass peaks, 695.3 $(M+H)^+$ and 717.6 $(M+Na)^+$, by ESI-MS. These are identical to those of the chemically synthesized authentic standard compound. These results are consistent with the formation of a peptide bond between the carbonyl of the substrate amino acid (biotin-Met-5′-AMP) and the phenylalanine amino group of 5′-Phe-SS-GMPS-RNA and the subsequent reductive cleavage of this bond.

The Optimal Substrate for R180 Ribozyme

The sample I prepared and purified by Gottikh's method [22] was used for the original selection in our previous work [21]. The NMR, HPLC, and mass spectrometer analyses demonstrated that it contained approximately 2% other components (aminoacyl-5′-adenylate, AMP-2′,3′-bis(aminoacyl) diester, and other components). We repurified sample I by using a C18 reverse phase column to obtain pure *N*-biotinyl-methionyl-3′(2′)-AMP. We also synthesized *N*-biotinyl-methionyl-2′,3′-adenylate diester. Sample I, monoester, diester, and anhydride were all characterized by NMR, mass, and HPLC spectroscopy. The ^{31}P-NMR and HPLC spectra of these samples are shown in Figures 4A–4F. The ^{31}P-NMR spectra showed the characteristic chemical shift for phosphorus of the AMP-3′(2′) monoester (0.434 ppm and 0.297 ppm; Figure 4A) and AMP-5′-anhydride (−7.521 ppm; Figure 4C). The chemical shift for the phosphorus of a diester is 0.206 ppm. The sample I contained some diester (0.144 ppm) and a trace amount of anhydride (−7.529 ppm).

All of these compounds were tested for peptide bond-forming activity with clone 25 and R180 ribozymes. The reactions were performed in the presence of 100 μM

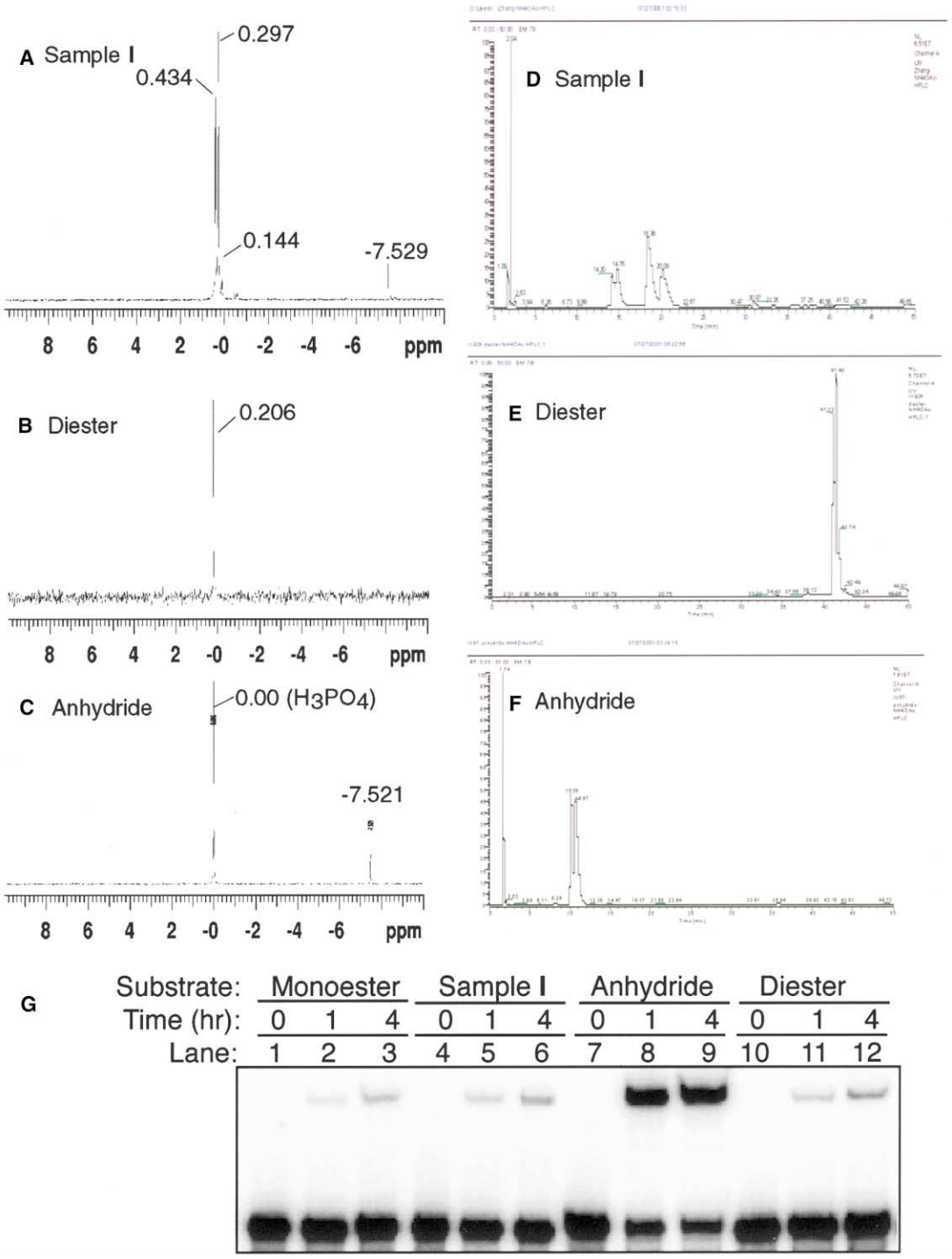

Figure 4. NMR, HPLC, and Activity Characterization of the Optimal Substrate for the R180 Ribozyme

^{31}P-NMR and HPLC spectra of sample I, AMP-2′,3′-bis(Met-Bio) diester, and *N*-biotinyl-methionyl-5′-adenylate anhydride (A–F). The ^{31}P-NMR spectra were taken in D_2O solvent, and phosphoric acid (H_3PO_4) was used as an external standard. Analytic HPLC conditions: C18 reverse-phase column (HyPURITY, ThermoQuest); 1.0 ml/min flow rate; eluted with 13% acetonitrile in 10 mM ammonium acetate buffer (pH 3.5). (G) Autoradiogram of the peptide bond-forming reactions by the R180 ribozyme with various substrates. 5′-Phe-SS-GMPS-RNA (1.0 μM) was incubated in 100 μM substrate with 100 mM $MgCl_2$ and 50 mM HEPES (pH 7.4) at 25°C. Monoester: *N*-biotinyl-methionyl-3′(2′)-adenylate; Sample I: the substrate used for selection in the previous study [21]; anhydride: *N*-biotinyl-methionyl-5′-adenylate; diester: AMP-2′,3′-bis(Met-Bio) diester.

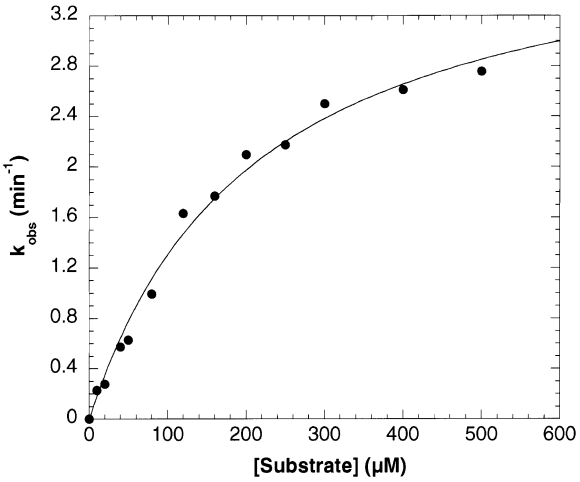

Figure 5. Michaelis-Menten Plot for the Peptide Bond-Forming Reaction of Biotin-Met-5′-AMP Catalyzed by R180 Ribozyme

Reactions were run in 0.5 μM R180 5′-Phe-SS-GMPS-RNA and 0–500 μM biotin-Met-AMP anhydride. The continuous line corresponds to the best-fit values of K_m and k_{cat}, obtained with the KaleidaGraph program.

substrate and 1.0 μM ribozyme in the reaction buffer at 25°C. The R180 ribozyme was highly active with the pure *N*-biotinyl-methionyl-5′-AMP anhydride (lanes 7–9, Figure 4G), as expected because it was selected for reaction with this substrate. It also showed low activity with pure *N*-biotinyl-methionyl-3′(2′)-AMP monoester (lanes 1–3), with sample I (lanes 4–6), and with *N*-biotinyl-methionyl-2′,3′-AMP diester (lanes 10–12). In contrast, the previously isolated clone 25 ribozyme is most active with sample I but also shows low reactivity with *N*-biotinyl-methionyl-5′-AMP anhydride (R.L.G., Z.C., L.S., B.Z., and T. Cech, unpublished data). In conclusion, *N*-biotinyl-methionyl-5′-AMP is an excellent substrate for the R180 ribozyme but not an optimal substrate for clone 25 ribozyme (Z. C., L.S., and B.Z., unpublished data).

Kinetic Analysis

Kinetic studies of the R180 ribozyme were performed with a fixed concentration of the ribozyme and various concentrations of biotin-Met-5′-AMP anhydride. A typical kinetic plot is shown in Figure 5. The ribozyme demonstrated behavior similar to the saturation kinetics of classical protein enzymatic catalysis. By fitting the data to the Michaelis-Menten equation, we obtained best-fit values of $k_{cat} = 4.05\ min^{-1}$ and $K_m = 210 \pm 26$ μM at pH 7.4 and 25°C. The apparent second-order rate constant, k_{cat}/K_m, equals 19,300 $M^{-1}{\cdot}min^{-1}$. Thus, compared to that of many protein enzymes, the catalytic efficiency of the R180 ribozyme is modest. Kinetic studies of the noncleavable 5′-Phe-NH$(CH_2)_6$NHC(O)CH_2-GMPS-RNA with biotin-Met-5′-AMP anhydride gave $k_{cat} = 4.72\ min^{-1}$ and $K_m = 1.04$ mM. The observed catalytic rates for both linkers were similar, but the K_m for the noncleavable linker was about five times higher than that of the native linker ribozyme, suggesting that the linker of 5′-Phe-linker-RNA affects the equilibrium binding constant of the substrate rather than the rate of the chemical step.

The length of the linker at the aminoacyl acceptor site was also critical for the peptide bond-forming reaction. Activity dramatically decreased or ceased when a shorter or longer linker was substituted (our unpublished data). A particular length of linker is probably required for proper positioning of the 5′-amino group of 5′-Phe-SS-RNA and its biotin-Met-5′-AMP substrate in the active site of the ribozyme.

Amino Acid Specificity

Non-ribosomal peptide synthesis and polyketide biosynthesis use an exceedingly diverse group of precursors for assembling peptide and polyketide compounds [27]. To establish the specificity of the R180 peptidyl transferase ribozyme, we studied the peptide bond-forming reactions of a series of biotin-aminoacyl-5′-AMP anhydrides with different 5′-aminoacyl′-SS-GMPS-RNAs. In order to examine amino acid specificity at both donor and acceptor sites, we prepared six biotin-aminoacyl-AMP anhydrides (aminoacyl: methionine [Met], leucine [Leu], glutamine [Gln], phenylalanine [Phe], arginine [Arg], and alanine [Ala]) and five 5′-aminoacyl′-SS-GMPS-RNAs (aminoacyl′: Phe, Leu, Gln, tryptophan [Trp], and lysine [Lys]). 5′-aminoacyl′-SS-GMPS-RNAs were prepared by a two-step chemical linkage from 5′-GMPS-RNA: in brief, the in vitro-transcribed 5′-GMPS-RNA was reacted with *N,N*′-bis(bromoacetyl)-cystamine and then treated with DTT to yield 5′-cysteamine-GMPS-RNA that was coupled with aminoacyl′-pyridyldithioethyl amide to produce 5′-aminoacyl′-SS-GMPS-RNA (the detailed synthesis will be described elsewhere).

The ribozyme-mediated reactions of six biotin-aminoacyl-AMP anhydrides with five 5′-aminoacyl′-SS-GMPS-RNAs were studied. Surprisingly, all six aminoacyl donors were actively used by the R180 ribozyme, and the activity observed in each case was quite similar. The rate constants for all 30 reactions catalyzed by the R180 ribozyme are listed in Table 1. The observed rate constant of the reaction of 50 μM biotin-Met-5′-AMP with 0.5 μM 5′-Phe-SS-GMPS-RNA was 0.76 min^{-1} (entry 1, Table 1). It was 0.022 min^{-1} for the combination of biotin-Phe-5′-AMP with 5′-Gln-SS-GMPS-RNA (entry 14). The peptide bond-forming reaction of the prototypic combination (biotin-Met-5′-AMP and 5′-Phe-SS-GMPS-RNA) was the fastest, but it was only 35-fold faster than the rate of the slowest combination, viz. 5′-Gln-SS-GMPS-RNA with biotin-Phe-5′-AMP. The rate constants of 21 combinations of 5′-aa′-SS-GMPS-RNA with biotin-aa-5′-AMP were between 0.11 min^{-1} and 0.37 min^{-1}, a range of less than 4-fold. The order of the peptide bond-forming activity of the aminoacyl donor was Met > Ala ≈ Gln ≈ Arg > Leu ≈ Phe, but the range of the relative rates was less than 8-fold. The biotin-Gln-5′-AMP and biotin-Arg-5′-AMP, both having polar chains, were better substrates than biotin-Phe-5′-AMP and biotin-Leu-5′-AMP, with their aromatic and aliphatic side chains, respectively. However, the best substrate was biotin-Met-5′-AMP, with a linear neutral side chain. These results suggest that the steric nature of the side chain may be a more important factor than the hydrophilicity at the aminoacyl donor site. Among the aminoacyl ac-

Table 1. The Observed Rate Constants of Five 5′-Aminoacyl-SS-GMPS-RNAs with Six Biotin-Amidocaproyl-Aminoacyl-AMP Phosphoanhydrides

Entry	Substrate	Ribozyme	k_{obs} (min^{-1})	Relative Rate
1	**Biotin-Met-AMP**		**0.76 ± 0.18**	**1.00**
2	Biotin-Phe-AMP		0.20 ± 0.06	0.26
3	Biotin-Leu-AMP	5′-Phe-SS-GMPS-RNA	0.17 ± 0.05	0.22
4	Biotin-Gln-AMP		0.31 ± 0.05	0.41
5	Biotin-Arg-AMP		0.32 ± 0.03	0.42
6	Biotin-Ala-AMP		0.36 ± 0.02	0.47
7	Biotin-Met-AMP		0.19 ± 0.02	0.25
8	Biotin-Phe-AMP		0.027 ± 0.008	0.04
9	Biotin-Leu-AMP	5′-Lys-SS-GMPS-RNA	0.034 ± 0.007	0.05
10	Biotin-Gln-AMP		0.16 ± 0.02	0.21
11	Biotin-Arg-AMP		0.12 ± 0.01	0.16
12	Biotin-Ala-AMP		0.17 ± 0.02	0.22
13	Biotin-Met-AMP		0.17 ± 0.01	0.22
14	Biotin-Phe-AMP		0.022 ± 0.007	0.03
15	Biotin-Leu-AMP	5′-Gln-SS-GMPS-RNA	0.031 ± 0.005	0.04
16	Biotin-Gln-AMP		0.16 ± 0.02	0.21
17	Biotin-Arg-AMP		0.11 ± 0.02	0.14
18	Biotin-Ala-AMP		0.16 ± 0.03	0.21
19	Biotin-Met-AMP		0.36 ± 0.03	0.47
20	Biotin-Phe-AMP		0.089 ± 0.017	0.12
21	Biotin-Leu-AMP	5′-Leu-SS-GMPS-RNA	0.076 ± 0.019	0.10
22	Biotin-Gln-AMP		0.23 ± 0.02	0.30
23	Biotin-Arg-AMP		0.19 ± 0.02	0.25
24	Biotin-Ala-AMP		0.17 ± 0.003	0.22
25	Biotin-Met-AMP		0.27 ± 0.01	0.36
26	Biotin-Phe-AMP		0.037 ± 0.009	0.05
27	Biotin-Leu-AMP	5′-Trp-SS-GMPS-RNA	0.040 ± 0.010	0.05
28	Biotin-Gln-AMP		0.17 ± 0.04	0.22
29	Biotin-Arg-AMP		0.14 ± 0.01	0.18
30	Biotin-Ala-AMP		0.17 ± 0.04	0.22

All reactions were performed with 0.5 μM 5′-aa-SS-GMPS-RNA and 50 μM biotin-aminoacyl-AMP in the presence of 300 KCl, 100 $MgCl_2$ and 50 mM HEPES (pH 7.4) at 25°C. Rate constants were obtained by averaging three or more kinetic runs. Other conditions are as described in the Experimental Procedures. Entry 1 (bold) is the prototype ribozyme.

ceptors, Phe was the best, and four other acceptors (Lys, Leu, Gln, and Trp) displayed little difference, from polar Gln and Lys to the nonpolar Leu and Trp. It is clear that the aminoacyl acceptor site of the ribozyme can accept several different classes of amino acids.

The kinetic analysis of reactions with the different amino acid substrates suggests that the active site of R180 ribozyme can accommodate positively charged arginine and lysine, polar glutamine, aromatic phenylalanine and tryptophan, and aliphatic alanine, leucine, and methionine residues. The AMP moiety of biotin-aminoacyl-5′-AMP anhydride may make a major contribution to the binding energy of the substrate with the R180 ribozyme discussed here, but it is also possible that the biotin moiety of the substrate interacts strongly with the ribozyme. In any case, our results suggest that the amino acid side chain of the substrate is not a major contributor to the substrate binding energy. The wide range of aminoacyl substrates showing similar activity is a remarkable feature of the R180 ribozyme.

In summary, the results of this investigation indicate that the R180 ribozyme: (i) effectively catalyzes dipeptide synthesis; (ii) has little specificity for either donor or acceptor amino acid; and (iv) utilizes as its preferred substrate the same intermediate employed in modern peptide biosynthesis, viz. the aminoacyl-5′-adenylate.

Significance

This study has potential implications regarding the origin and evolution of protein synthesis. We have isolated a ribozyme that can catalyze peptide bond formation between substrates that contain a variety of different amino acid residues. It may be analogous to modular peptide synthetases in non-ribosomal peptide synthesis. These synthetases employ exceedingly diverse groups of substrates, including hydroxyl, *N*-methylated, and D-amino acids. This ribozyme can utilize substrates analogous to the aminoacyl 5′-adenylate anhydrides that are universal, activated intermediates used by all living systems in both uncoded and coded biosynthesis of peptides or proteins. In light of a previous report that ribozymes can synthesize an aminoacyl-RNA anhydride [15], they may be able to catalyze the aminoacyl-adenylation reaction (Equation 1). Therefore, RNA might have functioned as a catalyst in uncoded peptide synthesis during an early stage in the evolution of life (Equation 2).

$$\text{aa} + \text{ATP} \xrightarrow{\text{ribozyme}} \text{aa} - \text{AMP} + \text{PP}_i \quad (1)$$

$$\text{aa} - \text{AMP} + \text{aa} - \text{RNA} \xrightarrow{\text{ribozyme}} \text{peptide} - \text{RNA} + \text{AMP} \quad (2)$$

Modular polyketide or non-ribosomal peptide biosyn-

thesis is a perfect model for non-template biopolymer synthesis. We proposed that an uncoded peptide synthesis might mimic the polyketide synthesis. The R180 ribozyme may catalyze the first step in the reaction of the proposed uncoded peptide synthesis. Our findings provide support for the feasibility of the hypothesis that uncoded peptide synthesis may have been the evolutionary antecedent of coded peptide synthesis and may have been catalyzed by RNA. Our results combined with previous demonstrations strongly support a critical role for RNA catalysis in the early evolution of life.

Experimental Procedures

General Materials

^{1}H-NMR spectra were recorded on a Varian 300 or 400 MHz spectrometer. All spectra used the residual solvent peaks as reference signals. Chemicals, solvents, drying agents, and inorganic salts were obtained from Fisher Scientific, Acros Chemical, Sigma-Aldrich, and Fluka Chemical unless otherwise indicated. Anhydrous *N,N*-dimethyl formamide (DMF), tetrahydrofuran (THF), and methyl sulfoxide (DMSO) were obtained in Sure/Seal bottles from Aldrich Chemical. Guanosine-5′-monophosphorothioate (GMPS) was purchased from EMP Biotech GmbH, Germany. The restriction enzymes, dNTPs, NTPs, and AMV reverse transcriptase were purchased from Amersham, immobilized streptavidin and streptavidin from Pierce, glycogen and Taq DNA polymerase from Boehringer Mannheim, RNase-free DNase I from Promega, and α-^{32}P-ATP from NEN Lab. Aqueous buffers were prepared with autoclaved deionized water, and pH values were adjusted with 1 N HCl or 1 N NaOH.

Chemical Synthesis

N-bromoacetyl-*N′*-phenylalanyl-1,6-diaminohexane [Phe-NH$(CH_2)_6$NHC(O)CH_2Br] was synthesized by a synthetic route similar to that for Phe-NH$CH_2CH_2SSCH_2CH_2$NHC(O)CH_2Br described in the literature [21]. An excess of 1,6-hexanediamine was reacted with *t-Boc-L*-phenylalanyl-*N*-hydroxysuccinimide ester, coupled with bromoacetyl *N*-hydroxysuccinimide ester, and finally deprotected with trifluoroacetic acid to yield *N-L*-phenylalanyl-*N′*-bromoacetyl-1,6-diaminohexane [Phe-NH$(CH_2)_6$NHC(O)CH_2Br].

(*N-t-Boc-L-*Phenylalanyl)-1,6-Diaminohexane

To a solution of 1,6-diaminohexane (2.7 g, 23.23 mmol) and 2.0 ml of diisopropyl ethylamine in 100 ml of anhydrous DMF was added dropwise a solution of *t-Boc-L*-phenylalanyl-*N*-hydroxysuccinimide ester (1.5 g, 4.14 mmol) in 100 ml of DMF at room temperature. The mixture was stirred for two days at room temperature. After removal of the white precipitate, the solvent was evaporated under reduced pressure to dryness. The residue was dissolved in 200 ml of ethyl acetate and washed twice with saturated sodium bicarbonate, twice with water, and once with saturated brine. The organic layer was dried with anhydrous sodium sulfate, and the solvent was removed under reduced pressure. The crude product was purified by flash chromatography with silica gel (eluted with 10% methanol in methylene chloride) to give the pure desired product (98%). ^{1}H-NMR (300 MHz, DMSO-d_6): δ 1.12–1.20 (m, 6H), 1.25 (s, 9H), 2.75 (m, 2H), 2.82 (m, 2H), 2.95 (m, 2H), 4.15 (m, 1H), 6.82 (NH, 1H), 7.20 (m, aromatic, 5H), and 7.81 (NH, 1H).

(*N-t-Boc-L-*Phenylalanyl)-N′-Bromoacetyl-1,6-Diaminohexane

A solution of (*N-t-Boc-L*-phenylalanyl)-1,6-diaminohexane (1.47 g, 4.04 mmol) and bromoacetyl *N*-hydroxysuccinimide ester (1.5 g, 6.35 mmol) in 20 ml of anhydrous DMF was stirred for two days at room temperature. The reaction was monitored by TLC (5% MeOH in $CHCl_3$) After removal of the DMF by evaporation under reduced pressure, the residue was dissolved in chloroform, and any insoluble material was removed by filtration. The clear solution was loaded on a silica gel column and first eluted with chloroform and then eluted with 1% and then 2% methanol in chloroform to collect the pure product (1.9 g, 97%). ^{1}H-NMR (300 MHz, $CDCl_3$): δ 1.10–1.35 (m, 6H), 1.38 (s, 9H), 1.45 (m, 2H), 3.00 (m, 2H), 3.15 (m, 2H), 3.25 (m, 2H), 3.85 (s, 2H), 4.25 (m, 1H), 7.14–7.35 (m, 5H); mass spectrum (ESI), two equal-intensity mass peaks: m/e = 485 (M + 1) [^{35}Br] and 487(M + 3) [^{37}Br].

N-L-Phenylalanyl-N′-Bromoacetyl-1,6-Diaminohexane

The *N-t-Boc-L*-Phenylalanyl-*N′*-bromoacetyl-1,6-diaminehexane (1.9 g) was dissolved in 40 ml of anhydrous methylene chloride. The solution was cooled on an ice-water bath to 0°C–5°C. A 4 ml aliquot of trifluoroacetic acid was added dropwise. The mixture was stirred for 2 hr at 0°C–5°C, then warmed up to room temperature for 1 hr. The reaction was monitored by TLC (5% MeOH-$CHCl_3$). After evaporation of the solvent under reduced pressure, the solid compound was dissolved in 1% MeOH-$CHCl_3$ and purified by a flash silica gel column eluted with pure $CHCl_3$, followed by 1%–10% methanol in chloroform to give a pure product (1.25 g, 82.9%). ^{1}H-NMR (300 MHz, $CDCl_3$): δ 1.10–1.35 (m, 6H), 1.41 (m, 2H), 3.02 (m, 2H), 3.16 (m, 2H), 3.34 (m, 2H), 3.78 (s, 2H), 3.95 (m, 1H), 7.14–7.30 (m, 5H); mass spectrum (ESI), two equal-intensity mass peaks: m/e = 385 (M + 1) [^{35}Br] and 387(M + 3) [^{37}Br].

N-Biotinyl-Amidocaproyl-Methionyl-5′-Adenylate Anhydride

A 0.8 M HCl solution (138 μl) was added to a mixture of *N*-biotinylamidocaproyl-*L*-methionine (0.1 mmol) and adenosine-5′-monophosphate (0.11 mmol) in water (51 μl) and pyridine (572 μl) at 0°C. A solution of dicyclohexylcarbodiimide (2.6 mmol) in pyridine (600 μl) was added above solution. The mixture was stirred in an ice-water bath for 3.5 hr. After removal of the solid precipitation, the liquid solution was precipitated with acetone at −70°C and collected by centrifugation. The pellet was washed with ethyl ether (30 ml), dissolved in water at 0°C, and immediately applied to a C18 reverse-phase column and eluted with water/methanol (0%–50%). The desired fractions were evaporated quickly within 10 min by vacuum pump, and the aqueous solution was lyophilized to yield a pure white solid. ^{1}H-NMR (D_2O): δ 8.45 (m, 1H), 8.26 (m, 1H), 6.12 (d, *J* = 6.87 Hz, 1H), 4.74 (m, 1H), 4.57-4.46 (m, 3H), 4.36 (m, 2H), 4.21 (m, 2H), 3.25 (m, 1H), 3.09 (m, 2H), 2.96 (m, 1H), 2.72 (m, 1H), 2.52–2.39 (m, 2H), 2.25–1.89 (m, 9H), 1.68–1.22 (m, 12H); ^{31}P-NMR (D_2O): δ −7.52; ESI-MS (M-H): calculated 816.3, found 816.3. Other biotin-aminoacyl-AMP anhydrides were prepared as above. The compounds were characterized by NMR, HPLC, and mass spectrometry.

In Vitro Selection

The initial RNA pool was prepared from PCR-amplified DNA by in vitro transcription in the presence of GMPS: GTP = 8:1. The 5′-GMPS-RNA was purified by PAGE and then reacted with *N*-bromoacetyl-*N′*-phenylalanyl-cystamine. The selection cycles of 1 to 10 were performed in the previous study [21]. After the tenth cycle, the selection conditions were as follows: the 1–4 μM 5′-Phe-SS-RNA was incubated with 0.1–8.0 mM biotinoyl-amidocaproyl-methionyl-5′-AMP anhydride in the presence of 100 mM $MgCl_2$, 300 mM KCl, and 50 mM HEPES buffer (pH 7.4) at 25°C. The initial pool for this additional selection imported 800 pmol RNA with $\sim 10^7$ estimated different RNA molecules. The active 5′-Phe-SS-RNA molecules were converted to 5′-biotin-Met-Phe-SS-GMPS-RNA, reisolated by streptavidin-agarose, and used as RT-PCR templates for the next cycle of selection. The first three cycles of selection to use biotin-Met-5′-AMP (cycles 11–13) employed mutagenic PCR to introduce variants. After sixteen total cycles of selection, the final pool was cloned and sequenced to identify the most active ribozymes.

Nuclease Digestion

The enzymatic-digestion reactions were carried out with 5′- or 3′-labeled R180 RNA in the presence of the reaction buffer (20 mM Tris-HCl [pH 7.5], 100 mM KCl, and 50 mM $MgCl_2$) at 37°C. A total of 2 μl of 5′- or 3′-labeled RNA ($\sim 10^6$ CPM) solution was incubated with the reaction buffer for 10 min at 50°C, slowly cooled down to room temperature, and then incubated with 1 μl of the appropriate diluted RNase solution (nuclease S1 and RNase T1 from Roche; RNase T2 from Sigma; RNase V1 from Pharmacia Biotech). The digestion products were resolved by subjecting them to electrophoresis through 20% polyacrylamide/7.5 M urea denaturing gels.

Kinetics Assays

A 0.5–2.0 μM solution of the R180 ribozyme was preincubated with 100 mM $MgCl_2$, 300 mM KCl, and 50 mM HEPES buffer (pH 7.4) for 10 min at 50°C. The reactions were initiated by the addition of 2.0

μl aliquots of 0.1–5.0 mM biotin-Met-AMP in deionized H_2O. Aliquots (1.0–2.0 μl) of the reaction mixture were removed at specific time intervals, quenched with 2.5 μl of 50 mM HEPES (pH 7.4), 25 mM EDTA, and 90% formamide dye, and stored in dry ice. Each sample was incubated with 7.5 μg of streptavidin for 20 min at room temperature and then loaded on a 7.5 M urea/8% polyacrylamide gel. The fraction of product formation relative to total substrate and product at each time point was quantitated with a Molecular Dynamics PhosphorImager.

LC-MS Analysis

A 2 μM solution of Phe-SS-GMPS-RNA was preincubated in the presence of 300 mM KCl, 100 mM $MgCl_2$, and 50 mM HEPES (pH 7.4) for 10 min at 50°C. After slow cooling to room temperature, the reaction was initially incubated with 50 μM biotin-Met-5′-AMP substrate in a 1.0 ml solution of 100 $MgCl_2$, 300 KCl, and 50 mM HEPES (pH 7.4) at 25°C. Additional biotin-Met-AMP was added to the reaction mixture as successive 10 μl aliquots from a 0.5 mM stock mixture in five intervals every hour. The reaction mixture was extracted with phenol/chloroform twice and with chloroform once, then precipitated with 3 volumes of ethanol. The RNA pellet obtained by centrifugation was resuspended in deionized water. After treatment with DTT, the sample was used directly for LC-MS analysis. Instruments: Finnigan-MAT HPLC and Finnigan LCQ DUO. Analytic HPLC conditions: C18 reverse-phase column (HyPURITY, ThermoQuest); 500 μl/min flow rate; 10 mM acetic acid (pH 3.45); the gradients were 10%–40% acetonitrile/30 min, 40%–100% acetonitrile/5 min, and 100% acetonitrile/5 min. ESI-MS conditions: positive ion electrospray mode, 250°C capillary temperature, 17.0V capillary voltage, and −4.5kV spray voltage.

Acknowledgments

We thank Dr. T. Cech, Dr. T. Pederson, and Dr. M. Yarus for helpful comments on this manuscript. This work was supported by a Support Program for Medical Schools grant from the Howard Hughes Medical Institute, by a Biomedical Research Grant of the Worcester Foundation, and by the University of Massachusetts Medical School Start-up Fund. R.L.G. was a Howard Hughes Medical Institute Predoctoral Fellow.

Received: December 28, 2001
Revised: March 15, 2002
Accepted: March 22, 2002

References

1. Woese, C.R. (1967). The Genetic Code: The Molecular Basis for Genetic Expression. (New York: Harper & Row), pp. 179–195.
2. Crick, F.H.C. (1968). The origin of the genetic code. J. Mol. Biol. *38*, 367–379.
3. Orgel, L.E. (1968). Evolution of the genetic apparatus. J. Mol. Biol. *38*, 381–393.
4. Gilbert, W. (1986). The RNA world. Nature *319*, 618–620.
5. Joyce, G.F., and Orgel, L.E. (1999). Prospects for understanding the origin of the RNA world. In The RNA World, R.F. Gesteland, T.R. Cech, and J.F. Atkins, eds. (Cold Spring Harbor, New York: Cold Spring Harbor Laboratory Press), pp. 49–77.
6. Schimmel, P., and Henderson, B. (1994). Possible role of aminoacyl-RNA complexes in noncoded peptide synthesis and origin of coded synthesis. Proc. Natl. Acad. Sci. USA *91*, 11283–11286.
7. Hager, A.J., Pollard, J.D., and Szostak, J.W. (1996). Ribozymes: aiming at RNA replication and protein synthesis. Chem. Biol. *3*, 717–725.
8. Yarus, M. (1999). Boundaries for an RNA world. Curr. Opin. Chem. Biol. *3*, 260–267.
9. Johnston, W.K., Unrau, P.J., Lawrence, M.S., Glasner, M.E., and Bartel, D.P. (2001). RNA-catalyzed RNA polymerization: accurate and general RNA-templated primer extension. Science *292*, 1319–1325.
10. Benner, S.A., Ellington, A.D., and Tauer, A. (1989). Modern metabolism as a palimpsest of the RNA world. Proc. Natl. Acad. Sci. USA *86*, 7054–7058.
11. Schimmel, P., Giege, R., Moras, D., and Yokoyama, S. (1993). An operational RNA code for amino acids and possible relationship to genetic code. Proc. Natl. Acad. Sci. USA *90*, 8763–8768.
12. Bodley, J.W. (1988). Protein metabolism. In Biochemistry, G. Zubay, ed. (New York: Macmillan Publishing Company), pp. 928–973.
13. Von Dohren, H., Keller, U., Vater, J., and Zocher, R. (1997). Multifunctional peptide synthetases. Chem. Rev. *97*, 2675–2705.
14. Marahiel, M.A., Stachelhaus, T., and Mootz, H.D. (1997). Modular peptide synthetases involved in nonribosomal peptide synthesis. Chem. Rev. *97*, 2651–2673.
15. Kumar, R.K., and Yarus, M. (2001). RNA-catalyzed amino acid activation. Biochemistry *40*, 6998–7004.
16. Illangasekare, M., Sanchez, G., Nickles, T., and Yarus, M. (1995). Aminoacyl-RNA synthesis catalyzed by an RNA. Science *267*, 643–647.
17. Illangasekare, M., and Yarus, M. (1999). Specific, rapid synthesis of Phe-RNA by RNA. Proc. Natl. Acad. Sci. USA *96*, 5470–5475.
18. Illangasekare, M., and Yarus, M. (1999). A tiny RNA that catalyzes both aminoacyl-RNA and peptidyl-RNA synthesis. RNA *5*, 1482–1489.
19. Wiegand, T.W., Jassen, R.C., and Eaton, B.E. (1997). Selection of RNA amide synthases. Chem. Biol. *4*, 675–683.
20. Lohse, P.A., and Szostak, J.W. (1996). Ribozyme-catalysed amino-acid transfer reactions. Nature *381*, 442–444.
21. Zhang, B., and Cech, T.R. (1997). Peptide bond formation by *in vitro* selected ribozymes. Nature *390*, 96–100.
22. Gottikh, B.P., Krayevsky, A.A., Tarussova, N.B., Purygin, P.P., and Tsilevich, T.L. (1970). The general synthetic route to amino acid esters of nucleotides and nucleoside-5′-triphosphates and some properties of these compounds. Tetrahedron *26*, 4419–4433.
23. Wickramasinghe, N.S.M.D., and Lacey, J.C., Jr. (1992). Mixed anhydrides are also formed in the esterification of 5′-AMP with N-acetylaminoacyl imidazolides: implications regarding the origin of protein synthesis. Orig. Life Evol. Biosph. *22*, 361–368.
24. Lacey, J.C., Jr., Thomas, R.D., Wicharamasinghe, N.S.M.D., and Watkins, C.L. (1990). Chemical Esterification of 5′-AMP occurs predominantly at the 2′-position. J. Mol. Evol. *31*, 251–256.
25. Berg, P. (1958). The chemical synthesis of amino acyl adenylates. J. Biol. Chem. *233*, 608–611.
26. Zuker, M., Mathews, D.H., and Turner, D.H. (1999). Algorithms and Thermodynamics for RNA Secondary Structure Prediction: A Practical Guide. In RNA Biochemistry and Biotechnology, J. Barciszewski and B.F.C. Clark, eds. NATO ASI Series, (Dordrecht, The Netherlands: Kluwer Academic Publishers), pp. 11–43.
27. Kleinkauf, H., and von Dohren, H. (1990). Nonribosomal biosynthesis of peptide antibiotics. Eur. J. Biochem. *192*, 1–15.